



## Large Eddy Simulation in Duct Flow

Jalal M. Jalil\*

Ihab Omar Abbas\*\*

\*,\*\* *Department of Machine and Equipment Engineering / University of Technology*

\* E-mail: [jalalmjalil@yahoo.com](mailto:jalalmjalil@yahoo.com)

\*\* E-mail: [ihabomar88@yahoo.com](mailto:ihabomar88@yahoo.com)

(Received 26 April 2015; accepted 22 March 2015)

### Abstract

In this paper, the problem of developing turbulent flow in rectangular duct is investigated by obtaining numerical results of the velocity profiles in duct by using large eddy simulation model in two dimensions with different Reynolds numbers, filter equations and mesh sizes. Reynolds numbers range from (11,000) to (110,000) for velocities (1 m/sec) to (50 m/sec) with (56×56), (76×76) and (96×96) mesh sizes with different filter equations. The numerical results of the large eddy simulation model are compared with k-ε model and analytic velocity distribution and validated with experimental data of other researcher. The large eddy simulation model has a good agreement with experimental data for high Reynolds number with the first, second and third mesh sizes and the agreement increase near the wall of the duct. The percentage error for the large eddy simulation model with experimental data of the (56×56) mesh size is less than 18 % and for the (76×76) mesh size is also less than 17% and for the (96×96) mesh size is less than 16 %. The large eddy simulation model show high stability and do not need extra differential equation like the k-ε model and a great saving in time and computer memory was achieved.

**Keywords:** *Large-eddy simulation, turbulence model, computational fluid-dynamics.*

### 1. Introduction

The turbulent flow is a flow regime described by chaotic and stochastic property changes; this involves low momentum diffusion, high momentum convection, and rapid variation of pressure and velocity in space and time. Until now no expected theory has been established which might be used with success to the vast variety of turbulent flows confronted in practice and consequently the treatment of most of these flows is counted on theoretical and numerical approximations. Some of these models are k-ε, large eddy simulation (LES), Reynolds averaged Navies-Stokes (RANS) and direct numerical simulation (DNS). G. Mompean [1] performed a numerical simulation with the non-linear turbulence model coupled with the k-ε equations. The fully developed turbulent flow through a straight square duct, including secondary motion, was simulated. L. C. Demartini, et al., [2] presented the numerical and experimental analysis of the turbulent flow of air inside a channel of

rectangular section, involving two rectangular baffle plates. M. Taeibi-Rahni, et al., [3] applied an eddy-viscosity sub grid-scale model in large-eddy simulation at Re=4700 of a film cooling flow. The model requires only a single-level test filter, and therefore was more appropriate for large-eddy simulation (LES) in complicated geometries. T. S. Lund [4] used explicit filtering in large eddy simulation (LES) with finite-difference methods. The idea that the finite-difference expressions act as an effective filter was shown to be false for three-dimensional simulations performed on nonuniform meshes. Michele Ciofalo,[5] discussed Large-eddy simulation (LES) results for the turbulent flow with heat transfer in different geometrical configurations, involving a plane channel, a channel bearing transverse square ribs on one of the walls, and a crossed-corrugated air heater. Mingde Su, et al., [6] used the Smagorinsky sub grid-scale model, a dynamic sub grid-scale model, and a stimulated sub grid-scale model to compute airflow in a room in a large eddy simulation (LES)

program. The present work is to investigate the problem of turbulent developing flow in rectangular duct by using large eddy simulation model in two dimensions with different Reynolds number, filter equations and mesh sizes and compare the results with the k-ε model and analytic velocity distribution and experimental data of other researcher.

## 2. Theoretical concept

During the last two decades there has been great interest in developing computational fluid dynamics (CFD) computer programs for predicting the air flow. The majority of these CFD programs are counted on the solution of Navier–Stokes equations, the energy equation, the mass and concentration equations as well as the transport equations for turbulent velocity and its scale [7].

### 2.1. Prandtl Mixing length

The mixing length (l) is introduced as the average lateral distance through which a small mass of fluid particles would move from one layer to the other adjacent layers before getting the velocity of the new layer. Prandtl assumed that components  $u'$  and  $v'$  are of the same order and the velocity fluctuation in X-direction is related to the mixing length [8].

$$\bar{\tau} = \rho \overline{u'v'} \quad \dots (1)$$

$$u' = l \frac{du}{dy} \quad \dots (2)$$

$$\overline{u' \times v'} = \overline{u' v'} = \left( l \frac{du}{dy} \right) \left( l \frac{du}{dy} \right) = l^2 \left( \frac{du}{dy} \right)^2 \quad \dots (3)$$

$$v' = l \frac{du}{dy} \quad \dots (4)$$

Substituting the value of  $\overline{u' v'}$  in eqn. (1), we get

$$\bar{\tau} = \rho l^2 \left( \frac{du}{dy} \right)^2 \quad \dots (5)$$

By neglect viscous shear stress

$$\frac{u}{u_m} = \left( \frac{y}{r_0} \right)^n \quad \dots (6)$$

### 2.2. Basic Governing Equations

The conservation equations for continuity, momentum, and energy equations and turbulence model can be written as follows [9]:

### Conservation of Mass (Continuity equation)

The change in mass flow within a control volume should be equal to the mass flow in minus the mass flow out through the control volume surfaces, since mass cannot be created or destroyed. This can be expressed mathematically for an incompressible fluid as:

$$\frac{\partial u}{\partial x} + \frac{\partial v}{\partial y} = 0 \quad \dots (7)$$

Navier-Stokes Equations (Momentum equation):

The momentum equations that govern the flow of fluid are concluded from the second law of motion by Newton (the conservation of momentum). The equations are called Navier-Stokes equations, two dimensions, non-uniform and incompressible fluid takes the form:

$$\rho \left( \frac{\partial(uu)}{\partial x} + \frac{\partial(vu)}{\partial y} \right) = -\frac{\partial p}{\partial x} + 2 \frac{\partial}{\partial x} \Gamma \frac{\partial u}{\partial x} + \frac{\partial}{\partial y} \Gamma \frac{\partial u}{\partial y} + \frac{\partial}{\partial y} \Gamma \frac{\partial v}{\partial x} \quad \dots (8)$$

$$\rho \left( \frac{\partial(uv)}{\partial x} + \frac{\partial(vv)}{\partial y} \right) = -\frac{\partial p}{\partial y} + \frac{\partial}{\partial x} \Gamma \frac{\partial v}{\partial x} + 2 \frac{\partial}{\partial y} \Gamma \frac{\partial v}{\partial y} + \frac{\partial}{\partial x} \Gamma \frac{\partial u}{\partial y} \quad \dots (9)$$

### 2.3. The k-ε Turbulence Model

The k-ε turbulence model is counted on the solution of equations for the turbulent kinetic energy and the turbulent dissipation rate.

The distribution of eddy viscosity throughout the flow domain should be organized in order to compute the momentum and heat diffusion coefficients for turbulent equations. This is the function of the turbulence model. The turbulence models implicitly establish the related strength of turbulent and molecular diffusion by computing the  $\mu_t$  distribution, the turbulence models implicitly establish the relative strength of turbulent and molecular diffusion [10].

The eddy viscosity is related to magnitudes of turbulence kinetic energy (k) and the dissipation rate of turbulence energy (ε) at each grid point:

$$\mu_t = \frac{C_D \rho k^2}{\epsilon} \quad \dots (10)$$

Where  $C_D$  is the empirical constant. The turbulent energy is known by the fluctuation velocities

$$k = \frac{1}{2} (\overline{u'^2} + \overline{v'^2})$$

The local distribution of  $k$  and  $\epsilon$  demand the solution of two additional transport equations, which are divided from the Navier-Stokes equation. The  $k$  transport equation is presented by:

$$\frac{\partial}{\partial x}(\rho uk) + \frac{\partial}{\partial y}(\rho vk) = \frac{\partial}{\partial x} \Gamma_k \left( \frac{\partial k}{\partial x} \right) + \frac{\partial}{\partial y} \Gamma_k \left( \frac{\partial k}{\partial y} \right) + G_k - \rho \epsilon \quad \dots (11)$$

$$G_k = \mu_t \left[ 2 \left( \left( \frac{\partial u}{\partial x} \right)^2 + \left( \frac{\partial v}{\partial y} \right)^2 \right) + \left( \frac{\partial u}{\partial y} + \frac{\partial v}{\partial x} \right)^2 \right] \dots (12)$$

The  $\epsilon$  equation is given by:

$$\frac{\partial}{\partial x}(\rho u \epsilon) + \frac{\partial}{\partial y}(\rho v \epsilon) = \frac{\partial}{\partial x} \Gamma_\epsilon \left( \frac{\partial \epsilon}{\partial x} \right) + \frac{\partial}{\partial y} \Gamma_\epsilon \left( \frac{\partial \epsilon}{\partial y} \right) + (C_1 G_k - C_2 \rho \epsilon) \frac{\epsilon}{K} \quad \dots (13)$$

### 2.4. Large Eddy simulation Model

Large-eddy simulation (LES), is a modelling technique that calculates for turbulent flows where the large, energy-carrying turbulent eddies are computed directly and the effect of the small-scale eddies below the computational grid size, which donate to the turbulence energy dissipation, are modeled through a sub grid-scale stress term. The large turbulent scales in LES are often distinguished from the small scales by using a spatial filtering process, which determines to what degree the large-scale eddy motions in a turbulent flow are explicitly resolved [7].

### 2.5. Smagorinsky Model

The Smagorinsky model is counted on the equilibrium hypothesis which implies that the small scales dissipate entirely and instantaneously all the energy they undergo from the large scales. LES calculations of concern are executed with equal mesh spacing in two spatial directions  $\Delta x$  and  $\Delta y$ .

The sub grid scale eddy viscosity, in this model, is related to the deformation of the resolved velocity field as:

$$\mu_t = (C_s \Delta)^2 |\bar{S}| \quad \dots (14)$$

Where

$$|\bar{S}| = [2 \bar{s}_{ij} \bar{s}_{ij}]^{\frac{1}{2}} \quad \dots (15)$$

$|\bar{S}|$  = is the magnitude of the strain-rate tensor.

$$\bar{s}_{ij} = \frac{1}{2} \left( \frac{\partial \bar{u}_i}{\partial x_j} + \frac{\partial \bar{u}_j}{\partial x_i} \right)$$

$\Delta$  = width filter

$$\Delta = (\Delta x \Delta y)^{1/2}$$

$C_s$  = Smagorinsky coefficient

The Smagorinsky coefficient  $C_s$ , in the present paper, is set equal to 0.17. This sub grid model largely employed in LES of isotropic turbulence presented good results. When it applied to homogeneous, and in particular to wall bounded flows, the constant was modified.

For two dimensions the magnitude of the strain-rate tensor will be:

$$|\bar{S}| = (2s_{xx}s_{xx} + 4s_{xy}s_{xy} + 2s_{yy}s_{yy})^{1/2} \quad \dots (16)$$

Where

$$s_{xx} = \frac{1}{2} \left( \frac{\partial u}{\partial x} + \frac{\partial v}{\partial x} \right) \quad \dots (17)$$

$$s_{xy} = \frac{1}{2} \left( \frac{\partial u}{\partial y} + \frac{\partial v}{\partial x} \right) \quad \dots (18)$$

$$s_{yx} = \frac{1}{2} \left( \frac{\partial v}{\partial x} + \frac{\partial u}{\partial y} \right) = s_{xy} \quad \dots (19)$$

$$s_{yy} = \frac{1}{2} \left( \frac{\partial v}{\partial y} + \frac{\partial u}{\partial y} \right) \quad \dots (20)$$

### 2.6. Spatial Filtering

Filtering is a mathematical operation designed to move out a range of small scales from the solution to the Navier-Stokes equations in the context of large eddy simulation (LES). Turbulent flows comes from the wide range of length and time scales because the principal difficulty in modeling, this operation produces turbulent flow modeling cheaper by decreasing the range of scales that should be resolved. The LES filter operation is low-pass, meaning it separates out the scales accompanied with high frequencies.

The filter that used in the program is box filter and the equation of box filtering for two dimensions for fig. (1) as below [11]:

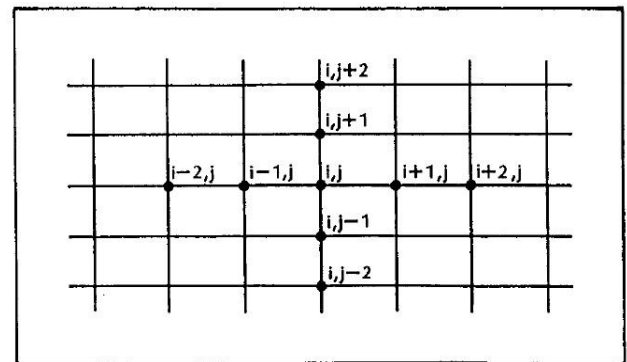


Fig. 1. Grid points for two dimensions.

$$f_{i,j} = (f_{i,j} + f_{i+1,j} + f_{i+2,j} + f_{i-1,j} + f_{i-2,j} + f_{i,j+1} + f_{i,j+2} + f_{i,j-1} + f_{i,j-2})/9 \quad \dots (21)$$

Others equation of box filtering are:

$$f_{i,j} = (f_{i+1,j} + f_{i+2,j} + f_{i-1,j} + f_{i-2,j} + f_{i,j+1} + f_{i,j+2} + f_{i,j-1} + f_{i,j-2})/8 \quad \dots (22)$$

$$f_{i,j} = (2f_{i+1,j} + f_{i+2,j} + 2f_{i-1,j} + f_{i-2,j} + 2f_{i,j+1} + f_{i,j+2} + 2f_{i,j-1} + f_{i,j-2})/12 \quad \dots (23)$$

$$f_{i,j} = (3f_{i+1,j} + f_{i+2,j} + 3f_{i-1,j} + f_{i-2,j} + 3f_{i,j+1} + f_{i,j+2} + 3f_{i,j-1} + f_{i,j-2})/16 \quad \dots (24)$$

$$f_{i,j} = (4f_{i,j} + f_{i+1,j} + f_{i+2,j} + f_{i-1,j} + f_{i-2,j} + f_{i,j+1} + f_{i,j+2} + f_{i,j-1} + f_{i,j-2})/12 \quad \dots (25)$$

$$f_{i,j} = (12f_{i,j} + 4f_{i+1,j} + f_{i+2,j} + 4f_{i-1,j} + f_{i-2,j} + 4f_{i,j+1} + f_{i,j+2} + 4f_{i,j-1} + f_{i,j-2})/32 \quad \dots (26)$$

### 3. Mesh Generation

The generation of computational mesh that is used for the discretized solution of two dimensional Navier-Stokes and continuity equations is three sizes of mesh as followed:

56×56

76×76

96×96

The partial differential equations fully describe duct air flow. However, the equations are non-linear and coupled. Numerical discretization techniques are presented to transform the problem to a solvable level. In essence, this includes approximating the governing differential equations by a system of algebraic relations. This is accomplished by subdividing the duct into finite volumes using a gridding system with the finite volume method. These located at the centers of the finite volumes rather than solving over the continuum pressures and velocities are expected only at discrete points.

FORTRAN version (4.00.5277) was used to solve the governing equations for flows through a two-dimensional duct based on finite volume method by an iterative method. The fig. (2) blow shows the Subroutine of les.

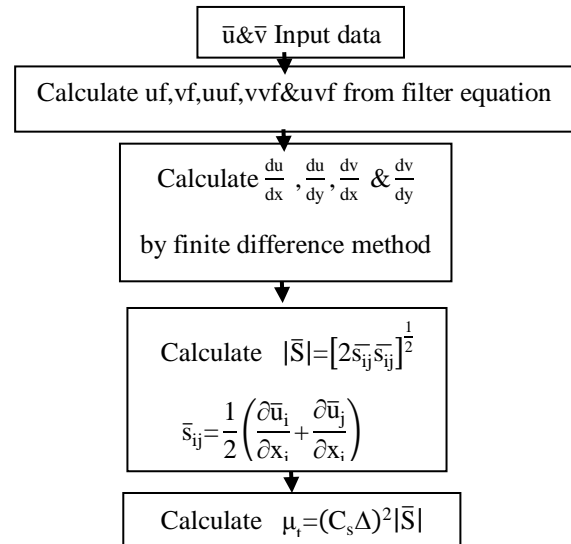


Fig. 2. Subroutine of les.

### 4. Boundary and Initial Condition of the Duct

The geometry considered is a duct model. The duct model has length up to 10 m and 0.127×0.127 m<sup>2</sup> cross section area. Fig. (3) shows basic dimensions of the duct geometry model. The boundary conditions used for the straight square rectangular duct is the velocity at the wall equal zero. The initial condition used for the straight square rectangular duct is different initial inlet velocities (2 to 11 m/sec) and the exit velocity is smooth exit.

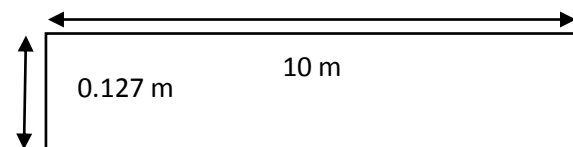


Fig. 3. Test duct dimensions.

### 5. Results and Discussion

In this paper, the results are presented to compare the velocity distribution for different numerical models inside rectangular duct of cross section area (0.127×0.127m<sup>2</sup>) and length of the duct up to (10 m). Results have been obtained for different Reynolds numbers, mesh sizes, and filter equations. The current numerical results are compared with the k- ε turbulence model and Prandtl mixing length numerical results, experimental results and the process that has been obtained from previous research for the purpose of validation.

### 5.1. Filter Equations

Velocity distribution was studied at Reynolds number (22300) with different filter equations (21 to 26).

The results obtained for velocity (3.3833 m/sec) at Reynolds number 22 300 for filter equations from (21) to (26) as shown in fig. (4).The result does not change for each filter equation.

The velocity profiles are similar to each other and there are no apparent effects of filter equation on these profiles that mean the average velocity for each control volume is equal. The change of the velocity profile for each velocity and Reynolds number carried out. The fig.(4) show the distribution of mean velocity between the half high of the square duct and the maximum velocity for different values of Reynolds number, where the Reynolds number is based on the inlet velocity and hydraulic diameter of the square duct. The profiles are strongly asymmetric and are appreciably dependent on Reynolds number.

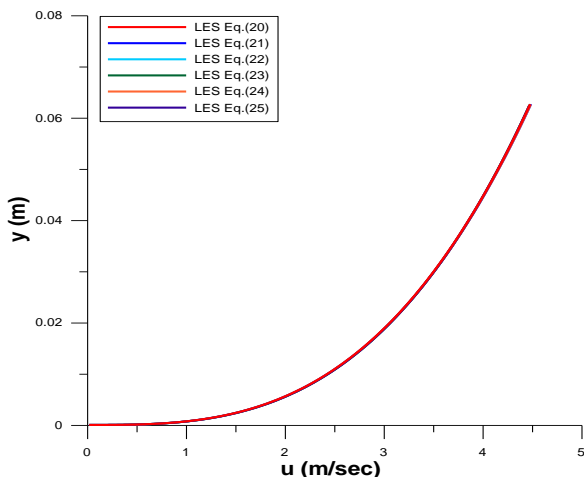


Fig. 4. Velocity distribution for different filter Eqs.at Re=22300.

### 5.2. Mesh Sizes

The velocity distribution was studied filter equation (21) with different mesh sizes (56×56), (76×76) and (96×96) at Reynolds number (34,300). These values were taken to compare the numerical results with the experimental data of Ref [12] for validation.

In fig (5), the comparison shows an acceptable agreement between the present work and published data for the (56×56), (76×76) and (96×96) mesh sizes. The difference between the experimental and numerical results at the (56×56)

mesh size was less than 18% and for the (76×76) mesh size was less than 17% and for (96×96) mesh size was less than 16%.

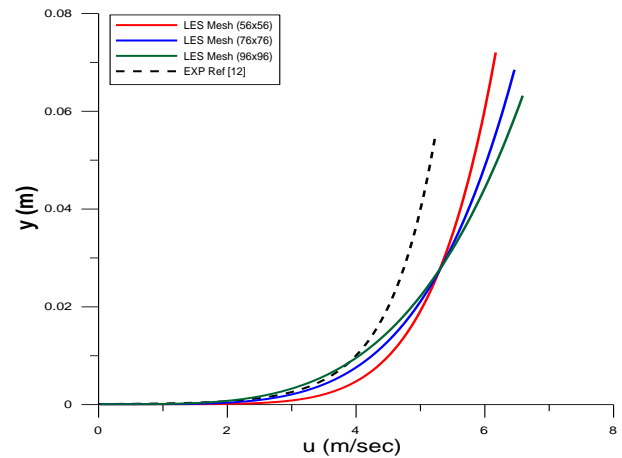


Fig. 5. Velocity distribution for different mesh sizes at Re=34300.

Fig. (6) shows a comparison of velocity distribution obtained from eddy simulation, k-ε, analytical models respectively. The calculations were carried out at Re=34000 and mesh size (96×96).

The large eddy simulation model has a good agreement with the experimental data Ref [12] near the wall. The k-ε model and analytic velocity distribution are very close. The large eddy simulation model shows high stability for calculation than the k-ε model where there is no source of error came from the negative value under the square root that obtained .The large eddy simulation model does not need extra differential equation to solve with the momentum equation like k and ε equations.

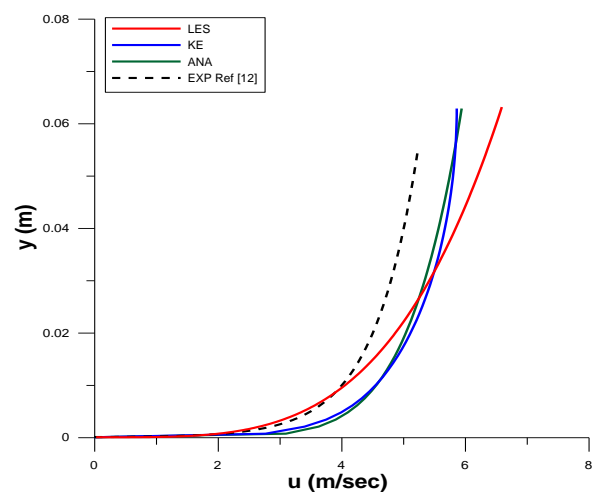


Fig. 6. Velocity distribution at Re=34,300 of (96 × 96) mesh size.

## 6. Conclusions

From the results of the present work, the following conclusions are deduced:

1. The filter equation does not change the numerical results for all cases at different Reynolds numbers.
2. The agreement of the velocity distribution between the large eddy simulation model and the experiment data of Ref [12] increase with increase of Reynolds number.
3. The agreement of the velocity distribution between the large eddy simulation model and the experiment data of Ref [12] increase with increase of the mesh generation.
4. Large eddy simulation model has a good agreement with the experimental data Ref [12] near the wall.

## Nomenclature

$u',v'$	Fluctuations, lateral and vertical velocity components respectively	$m/s$
$l$	Mixing length	$m$
$U_m$	Maximum velocity	$m/s$
$u$	Instantaneous velocity	$m/s$
$r_o$	Radius of pipe	$m$
$y$	Depth of flow	$m$
$C_d$	Empirical constant	/
$k$	Turbulent kinetic energy	$m^2/s^2$
$G_k$	Generation rate of turbulence energy	/
$C_D$	Smagorinsky coefficient	/
$\Delta$	Width filter	$m$
$\varepsilon$	Turbulent energy dissipation rate	$m^2/s^2$
$\Gamma$	Diffusion coefficient	---
$\rho$	Density	$kg/m^3$
$\mu_t$	Eddy viscosity	$pa.m$
$\tau$	Shear stress	$pa$
	Subscripts	
$t$	turbulent	
$m$	Maximum	
$o$	outlet	

## 7. References

- [1] G. Mompean, "Numerical Simulation of A Turbulent Flow Near A Right-Angled Corner Using The Speziale Non-Linear Model With RNG K- $\varepsilon$  Equations", Computers & Fluids, Vol. 27, pp. 847-859, (1998).
- [2] L. C. Demartini, H. A. Vielmo and S. V. Möller, "Numeric and Experimental Analysis of the Turbulent Flow through a Channel With Baffle Plates", Journal of the Brazilian Society of Mechanical Sciences and Engineering, No. 2, (2004).
- [3] M. Taeibi-Rahni, M. Ramezanizadeh, D.D. Ganji, A. Darvan, E. Ghasemi, Soheil Soleimani, H. Bararnia, "Comparative study of large eddy simulation of film cooling using a dynamic global-coefficient sub grid scale eddy-viscosity model with RANS and Smagorinsky Modeling", International Communications in Heat and Mass Transfer, Volume 38, pp. 659-667, (2011).
- [4] T. S. Lund, "The Use of Explicit Filters in Large Eddy Simulation", International Journal of Heat and Mass Transfer, pp. 603-613, (2003).
- [5] Michele Ciofalo, "Large-eddy simulations of turbulent flow with heat transfer in simple and complex geometries using Harwell-Flow 3D", Applied Mathematical Modelling vol.20, pp 262–271 (1996).
- [6] Mingde Su, Qingyan Chen, Che-Ming Chiang, "Comparison of Different Sub grid-Scale Models of Large Eddy Simulation for Indoor Airflow Modeling", Journal of Fluids Engineering, Volume 123, pp. 628-639, (2001).
- [7] Hazim B. Awbi, "Ventilation of Buildings", Spon Press, 2th edition, (2005).
- [8] R.K. Rajput, "a Text Book of Fluid Mechanics and Hydraulics Machines", S.Chand & Company Ltd., (2008).
- [9] Sinan Mazin Hazim, "The Effect of Phase Change Material Section on the Convection Heat Transfer Coefficient", M.Sc. Thesis, Technical College/Baghdad (2011).
- [10] Nassir Ibraheem Khalaf, "Experimental and Numerical Analysis of Air Outlet Configuration in Air-Conditioned Space", M.Sc. Thesis, Technical college/Baghdad (2008).
- [11] Klaus A.Hoffmann, "Computational Fluid Dynamics for Engineerings", 4th edition, engineering education system, (1989).
- [12] Lawrence C. Hoagland "Fully Developed Turbulent Flow in Straight Rectangular Ducts -Secondary Flow, Its Cause and Effect On The Primary Flow", PhD thesis, Mechanical Engineering, Massachusetts Institute of Technology, (1960).

## محاكاة الدوامة الكبيرة لجريان داخل مجرى

جلال محمد جليل\* ايهاب عمر عباس\*\*

\*\*،\* قسم هندسة المكائن والمعدات / الجامعة التكنولوجية

\* البريد الالكتروني: [jalalmjalil@yahoo.com](mailto:jalalmjalil@yahoo.com)\*\* البريد الالكتروني: [ihabomar88@yahoo.com](mailto:ihabomar88@yahoo.com)

## الخلاصة

في هذا البحث تم دراسة تطور الجريان المضطرب دراسة نظرية عددية خلال مجرى مربع المقطع من خلال نتائج نظرية لتوزيع السرعة باستخدام نظرية محاكاة الدوامة الكبيرة ثنائية الابعاد لارقام رينولدز تتراوح من (11,000) الى (110,000) وسرع تتراوح من (1 m/sec) الى (50 m/sec) و معادلات تصفية مختلفة و شبكات مختلفة مثل الشبكات (56x56) و (76x76) و (96x96). النتائج النظرية لنموذج محاكاة الدوامة الكبيرة تم مقارنتها مع نماذجين اخرين (k-ε) للاضطراب والرموز التحليلي. تم ايضا مقارنة النتائج النظرية لنموذج محاكاة الدوامة الكبيرة مع النتائج المختبرية لباحث سابق وكانت النتائج تشير الى وجود تقارب جيد بين النظريتين العدديتين محاكاة الدوامة الكبيرة و نموذج للاضطراب والنتائج المختبرية لارقام رينولدز العالية نسبيا باستخدام الشبكة الاولى والثانية والثالثة ويزداد التقارب بالقرب من الجدار. علما ان النسبة المئوية للخطأ كانت اقل من 18% لنموذج محاكاة الدوامة الكبيرة مع النتائج المختبرية لنفس الباحث باستخدام الشبكة (56x56) وللشبكة (76x76) اقل من 17% ايضا. في حين كانت نسبة الخطأ باستخدام الشبكة (96x96) اقل من 16%. نظرية محاكاة الدوامة الكبيرة توضح استقرارية عالية ولا تحتاج متغيرات كثيرة ومعادلات تفاضلية اضافية للحل كما في نظرية (k-ε) كما توفر الوقت وسعة الذاكرة للحاسوب.